applied sciences

MDPI

Article

Hydrothermal Leaching of Silver and Aluminum from Waste Monocrystalline and Polycrystalline Photovoltaic Panels

Eleni Kastanaki, Emmanouel Lagoudakis, Georgios Kalogerakis and Apostolos Giannis *

School of Chemical and Environmental Engineering, Technical University of Crete, University Campus, 73100 Chania, Greece

* Correspondence: agiannis@tuc.gr

Abstract: The aim of this study was to investigate the hydrothermal leaching of silver and aluminum from waste monocrystalline silicon (m-Si) and polycrystalline silicon (p-Si) photovoltaic panels (PV) from both cells and metal ribbons using mild HNO_3 solutions. Prior to leaching, pretreatment was applied to remove the fluoropolymer backsheet and thermally degrade the ethyl vinyl acetate (EVA) polymer. Several hydrothermal parameters were investigated, such as the liquid-to-solid (L/S) ratio, HNO_3 concentration (N), time (t) and temperature (T). Based on preliminary tests, the HNO_3 concentration was set in the range of 1–2 N to reduce hazardous waste effluents. The response surface methodology (RSM) was applied to optimize the hydrothermal leaching parameters. It was found that processing time was the most important factor for Ag leaching, followed by HNO_3 concentration and L/S ratio, while the processing temperature (100–140 °C) was not a statistically significant factor. Aluminum leaching was efficient under most hydrothermal conditions. For comparison, leaching was also applied at lower temperatures of 25–45 °C for prolonged times; however, lower efficiencies were observed. Under the optimal hydrothermal conditions, Ag can be completely leached, while Al dissolution was favored at hydrothermal conditions compared with lower temperature leaching. Silver leaching efficiency was 100% under hydrothermal conditions; however, under conventional lower temperature conditions, it was 80.7–85.3% for m-Si and p-Si waste panels. Under conventional lower temperature conditions, Al leaching efficiency was 56.6–61.3% for p-Si and m-Si waste panels.

Keywords: crystalline silicon PV panels; silver; recycling; e-waste; response surface methodology

Citation: Kastanaki, E.; Lagoudakis, E.; Kalogerakis, G.; Giannis, A. Hydrothermal Leaching of Silver and Aluminum from Waste Monocrystalline and Polycrystalline Photovoltaic Panels. *Appl. Sci.* **2023**, *13*, 3602. https://doi.org/10.3390/app13063602

Academic Editor: Antonio Miotello

Received: 15 February 2023
Revised: 8 March 2023
Accepted: 8 March 2023
Published: 11 March 2023

1. Introduction

Due to the unprecedented worldwide increase in photovoltaic (PV) installations and considering the typical lifetime of PV panels of 25 years, there is a growing concern about emerging PV waste in the near future. It is estimated that 60–78 million tonnes (Mt) of PV waste will be generated worldwide by 2050, while in the EU-27 alone, PV waste will be 14.3–18.5 Mt. First-generation crystalline silicon (c-Si) modules have had a 80–90% market share over the last 40 years and will thus dominate the PV waste stream. Of these c-Si panels, 51% of the PV market share is covered by polycrystalline silicon (p-Si) and 41% is covered by monocrystalline silicon (m-Si) [1,2]. In the EU-27, c-Si panel waste was 90% until 2019 and is predicted to be 80–87% during 2020–2050 [3]. Thus, research on PV panel recycling should primarily focus on c-Si panels due to their large volume compared with other panel technologies.

Crystalline silicon PV modules consist of various types of materials such as glass, polymer layers of ethyl vinyl acetate (EVA), crystalline silicon cells, copper and silver metal contacts, a polymer backsheet and an aluminum frame. This layered design hinders the reuse of modules and restricts recycling options. The mass of a typical PV module is more than 90% glass, polymers and the aluminum frame [4,5]. However, there are also components in smaller proportions that require more attention, such as silver, tin, lead and other metals. Of these finite materials, silver and tin will be depleted in the

next 50 years, while other metals will last for another 50–500 years [2,6]. Although Ag is present in tiny amounts in PV panels, it contributes significantly to the revenue from recycled panel materials due to its high economic value [2]. According to Tao et al. [7], Ag represented 35.2% of the economic value derived from material recovery from a Si module in 2019. In the EU-27, the economic value of Ag will represent 17.6% of the total revenue from recycled materials by 2040, although its mass share in the accumulated PV waste (considering all PV technology waste) will be only 0.05% [3]. The average quantity of Ag in a PV panel is estimated at approximately 10 g per square meter. According to US resources, the Ag content should surpass 700 g/t when mined to be profitable as a primary product. As a result, Ag recovery from PV panel waste is becoming increasingly important [8–10]. Initially, research on PV panel recycling focused on silicon, glass and aluminum recovery [11,12]; however, more recent studies also aim at silver leaching and recovery [5,13].

In order to maximize Ag leaching efficiency, the operating parameters of temperature, time, L/S ratio and HNO_3 concentration should be optimized. This can be accomplished with appropriate statistical techniques, such as the response surface methodology (RSM) with a Box–Behnken design (BBD) [14]. This design investigates the effects of the parameters on silver leaching by simultaneously differentiating all parameters under consideration, instead of differentiating one parameter at a time. Thus, possible interactions between factors can be identified. The Box–Behnken design effectively avoids the realization of the complete experimental design, which would otherwise make the process more demanding in terms of time and resources, without losing any information on the effects of the parameters on the process. In this design, three levels of each factor are defined: low, middle and high [14,15]. Among the response surface designs, BBD is slightly more efficient compared to the central composite design, and is much more efficient than the three-level full factorial design [16]. This approach (RDM-BBD) is currently missing from the literature to optimize Ag leaching from waste PV panels.

The traditional acid-leaching process involves leaching metals from various matrices in non-pressurized hot water using mainly inorganic acids. In this process, the reaction temperature should be low in order to avoid water evaporation (<80–90 °C). The low leaching temperature requires a long reaction time, as well as a high acid concentration, to ensure complete leaching; however, this increases costs and environmental load [17–19]. Nonetheless, conventional acid leaching has been extensively applied to leach metals from waste PV panels [8,13].

Some studies also considered the leaching of Al along with Ag from PV cells [20,21]. Due to the high value of Ag, the main focus should be on this metal. The literature on the recycling of PV panels focuses on Ag recovery from cells, ignoring the ribbons [5,22]. However, significant amounts of Ag are adhered to the metal ribbons, and should be recovered and not lost. Currently, there is little research on Ag recovery from metal ribbons [21]; thus, this research gap should be filled. In previous studies, the most used method for Ag recovery from solar cells was etching or leaching in an acidic solution based on nitric acid (HNO_3) at concentrations of 2.3–14 N and temperatures of 25–80 °C. These experiments were performed in various vessels, with or without agitation [9,22]. Other studies used electrowinning of Ag with methanesulfonic acid solution as the electrolyte [23].

In contrast with traditional leaching methods, the hydrothermal leaching process is not limited by the boiling point of water at 100 °C. Using pressurized hot water as the solvent and with elevated temperatures, the hydrothermal method can efficiently leach metal ions from various matrixes. The high temperature accelerates the process, shortens the reaction time, and decreases the required acid concentration [24,25]. In this way, hydrothermal leaching is more efficient and environmentally friendly than traditional leaching methods [25,26]. Although hydrothermal leaching is a potential leaching method, so far, the process has not been utilized for PV waste, leaving a significant research gap to be filled. Hydrothermal metal leaching has been efficiently utilized for other types of waste, such as lithium-ion battery cathode materials [25], electroplating sludge [26]

and copper anode slime [27]. The efficient recovery of precious metals from waste PV panels under mild conditions is necessary to reduce the environmental impact and achieve financial benefits.

The present study fills this research gap using weak leaching agents to avoid the generation of hazardous waste effluents. Several hydrothermal experiments were performed, investigating the influence of four parameters on leaching efficiency: liquid to solid ratio (L/S), HNO_3 concentration (N), time (t) and temperature (T). To efficiently plan the experiments, the response surface methodology (RSM) with a Box–Behnken design was used.

The objectives of this study were: (i) to leach Ag and Al from both PV cells and ribbons, (ii) to investigate the influence of four parameters (L/S, HNO_3, t and T) on the hydrothermal leaching of Ag and Al, (iii) to compare hydrothermal with conventional leaching and (iv) to investigate the influence of milling and agitation on leaching efficiency.

2. Literature Review

Table 1 summarizes the leaching conditions used in various studies on Ag leaching from PV panels. These conditions refer to low-temperature acid leaching; there are no reported studies on hydrothermal leaching from waste PV panels. The most common method for Ag recovery from solar cells was etching/leaching in acidic solution using nitric acid (HNO_3). Various pretreatment techniques were applied for EVA removal, followed with milling and sieving. As seen in Table 1, the optimized HNO_3 concentration varies from 2.3 to 14 N, the temperature ranges from 25 to 80 °C and the time varies from 2 h to complete dissolution.

Table 1. Leaching conditions for Ag dissolution from PV panels.

Reference	Leaching Agent	Temperature (°C)	Time (h)
[9]	3 N HNO_3	50	3
[22]	90:10 methanesulfonic acid (99 wt.%):H_2O_2 (30 wt.%)	25	4
[5]	2.3 N HNO_3	55	2
[21]	5 N HNO_3	80	1
[13]	13.8 N HNO_3	25	2
[8]	2.6 N HNO_3	60	until complete dissolution

After successful leaching of Ag, the recovery of metallic Ag was achieved with electrochemical precipitation when the concentration in the solution was high enough [9], or with chemical precipitation and subsequent reduction of the silver. For the electrochemical silver precipitation, Oliveira et al. [5] processed 50 mL of leached solutions using a platinum plate (7 cm × 2 cm), a steel plate (7 cm × 2 cm) with a density of 60 A/cm^2, and a space between the electrodes of 30 mm for 1 h. For the chemical precipitation of Ag, 37% HCl was used. Then, AgCl was converted to Ag metal powder, first reacting with an aqueous NaOH solution (2% wt.) while stirring at 200 rpm for 1 h, followed with the addition of H_2O_2 (30% wt.) and a further reaction for 0.5 h. The recovered Ag metal powder was manufactured into an ingot using a thermal torch [22]. Alternatively, high purity Ag powder can be obtained with ammonia dissolution using a hydrazine hydrate reduction of the AgCl precipitate [28].

Various Al leaching conditions are also found in the literature. Theocharis et al. [20] reported that the use of 3 N HNO_3 for 2 h at 25 °C could quantitatively leach Al from PV powder and flakes. However, Chen et al. [21] leached 76% of Al using 5 N HNO_3 for 1 h at 80 °C, as the complete dissolution of Al was not possible due to Al–Si alloy formation. Since HNO_3 can also leach Ag, if Ag is to be electrowon, the simultaneous extraction of Al and Ag should be avoided. In this case, selective dissolution of Al can be accomplished with H_2SO_4 (12 M, 3 h, 25 °C) [20,29].

3. Materials and Methods

The raw materials in this research were waste monocrystalline silicon (m-Si) and polycrystalline silicon (p-Si) PV panels, collected from local PV trading/installation companies located in Chania and Heraklion, Greece, as described in [10]. Specifically, the p-Si panel (series SYP230S) was manufactured by Risen Energy Co. Ltd. and the m-Si panel (series ESP 60) was manufactured by ExelGroup Ltd. The operational lifetime of the panels was complete due to external damage caused by extreme weather conditions. However, their multilayered structure was not destroyed. The panels were stored in the laboratory until used in the experiments. Figure 1 shows pieces of m-Si and p-Si panels after removing the aluminum frames.

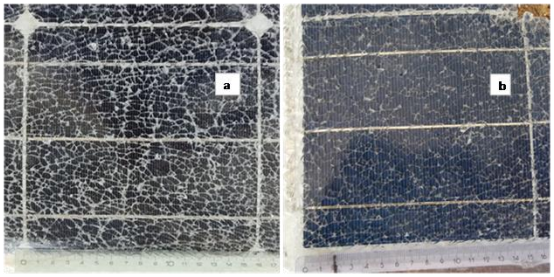

Figure 1. Pieces of: (**a**) m-Si and (**b**) p-Si panels after removing the aluminum frames.

3.1. Composition of c-Si Photovoltaic Modules

3.1.1. Pretreatment

The panels were initially dismantled and the aluminum frames, junction-boxes and cables were removed. Then, the panels were manually shredded with scissors and cutters into small pieces of approximately 4 × 4 cm^2. Before further treatment, the backsheets were manually removed. The backsheets consisted of layers of superposed fluorinated and terephthalate polymers (either polyvinyl fluoride or Tedlar film, and polyethylene terephthalate or PET, in the sequence: Tedlar, PET, Tedlar) [30].

The manual method was selected after preliminary thermal treatment tests. Some pieces with and without the backsheet were thermally treated with a Nabertherm furnace in an oxidizing atmosphere (600 °C 30 min). It was observed that a significant amount of ash was generated in the pieces with the fluoropolymer backsheet; however, almost no ash was generated in the pieces without the backsheet [31]. Thus, to avoid hazardous gas emissions of hydrofluoric acid and fluorinated compounds, and to ensure ease of handling, it was decided to manually remove the backsheet before further treatment [30]. During manual handling, it was observed that for some panel pieces, the back film was easily removed by hand, while for other pieces, a vise and saw were necessary. This could be due to non-uniform degradation of the EVA film due to weather conditions, as the backsheet was attached to an EVA film [32]. Thus, the possible degradation of EVA by weathering may facilitate the delamination of the backsheet, explaining why detachment was easier for some panel pieces.

3.1.2. Thermal Pretreatment of End-of-Life Si PV Panels

After removing the white backsheet, the panels were thermally treated to eliminate the EVA layer and thus separate the PV panels into glass, silicon cells and metal ribbons. The decomposition of the adhesive resin was carried out using a Nabertherm furnace in an oxidizing atmosphere. The samples were heated at 600 °C for 20 min.

After the thermal pretreatment, the panels were separated by screening with sieves of different sizes into glass, cells and metal ribbons. The glass was easily recovered and recycled. The separated cells, as well as the metal ribbons, were subjected to hydrothermal treatment.

3.1.3. Characterization of PV Panel Components

The separated cells and metal ribbons were separately milled with a Fritsch Pulverisette 19 mill equipped with a sieve of 0.5 mm and then subjected to X-ray fluorescence analysis (XRF, Spectro Xepos with software X-Lab Pro 4.0 and Turbo Quant screening method, Kleve, Germany) to determine their chemical composition. The results are presented in Table 2.

Table 2. Chemical composition of cells and ribbons.

Element (% *w*/*w*)	p-Si Cell	m-Si Cell	p-Si Ribbon	m-Si Ribbon
Si	64.46 ± 0.22	65.18 ± 0.31	2.78 ± 0.09	4.55 ± 0.13
Al	6.16 ± 0.05	9.87 ± 0.07	5.50 ± 0.05	5.59 ± 0.03
Cu	0.25 ± 0.02	0.93 ± 0.01	38.83 ± 0.11	48.51 ± 0.34
Ag	1.13 ± 0.02	1.37 ± 0.01	4.62 ± 0.06	6.22 ± 0.04
Sn	0.10 ± 0.03	0.28 ± 0.01	8.57 ± 0.06	10.68 ± 0.09
Pb	0.13 ± 0.03	0.35 ± 0.01	9.98 ± 0.05	10.13 ± 0.07

The gravimetric determination of the panel components was also carried out, taking into account EVA volatilization (Table 3). To ensure homogeneity and representativeness in each sample, a PV laminate of 15.8 × 15.8 cm^2 was quartered and the mass of glass, solar cells, metal ribbons and EVA was determined. Since significant amounts of silver were also found in the metal ribbons (Table 2), both cells and ribbons were used in the subsequent treatment. The proportion of cells to ribbons (Table 3) remained the same in all samples.

Table 3. Gravimetric determination of panel components.

Material	p-Si	m-Si
(% *w*/*w*)	Panel	Panel
glass	88.35 ± 0.18	89.37 ± 0.23
cell	5.25 ± 0.08	5.1 ± 0.20
ribbons	1.16 ± 0.01	0.98 ± 0.01
EVA	5.23 ± 0.11	4.56 ± 0.03

Losses due to milling were also calculated. For this reason, cells and ribbons were mixed in the proportions below (Table 3) and then milled. The resulting ground sample (a mixture of both cells and ribbons) was subjected to XRF analysis.

3.2. Experimental Design: Response Surface Methodology

Four different parameters (independent variables) of the hydrothermal leaching process were initially investigated: (i) temperature, (ii) time, (iii) L/S ratio and (iv) HNO_3 concentration. The effects of the independent variables on the leaching yield (dependent variable) were evaluated. In order to create an environmentally friendly process, low acid concentrations, short reaction times and relatively low reaction temperatures were used. The experimental design was performed with Minitab software and the input settings are presented in Table 4. All experiments were duplicated.

Table 4. Response surface methodology with a Box–Behnken experimental design.

Run Order	HNO_3 (N)	Time (min)	Temperature (°C)	L/S
1	1.5	120	120	10
2	1.5	75	100	20
3	1.5	75	120	15
4	2	120	120	15
5	1.5	75	100	10
6	1	30	120	15
7	1.5	30	140	15
8	1.5	30	100	15
9	1	75	120	20
10	1.5	120	140	15
11	1	75	100	15
12	1.5	30	120	20
13	1.5	75	120	15
14	2	75	120	20
15	1.5	120	120	20
16	2	30	120	15
17	1.5	75	140	10
18	2	75	140	15
19	2	75	100	15
20	1.5	120	100	15
21	1.5	75	120	15
22	1	120	120	15
23	1.5	75	140	20
24	2	75	120	10
25	1	75	120	10
26	1	75	140	15
27	1.5	30	120	10

3.3. Metal Leaching

As previously mentioned, prior to metal leaching the samples were milled. This facilitated cleavage of the chemical and mechanical bonds between the Ag and Al electrodes and the Si layer, and made the surface area for the reaction larger. To test the effect of milling, two samples were prepared: a powder sample (powder size < 0.5 mm) and a flake sample (random flakes of about 0.5–1 cm^2). Preliminary studies on silver leaching were carried out to screen the optimal conditions by determining the leaching agent (HNO_3) and its concentration range, the temperature and the contact time range. Silver can be easily dissolved in HNO_3 as the possible chemical reactions of Ag with HNO_3 have negative values of standard-state free energy (ΔG), indicating the spontaneous character of the reactions [33]. Since Ag is a more valuable metal compared to Al, choosing only one type of acid is considered the most profitable solution.

a. Hydrothermal leaching

Hydrothermal leaching tests were performed in cylindrical steel reactors (Techinstro, Nagpur, India) internally coated with PTFE and with a volume of 100 mL (Figure 2). The sample was mixed with 30 mL of HNO_3 according to the desired L/S ratio and was hydrothermally treated at 100–140 °C for 0.5–2 h without stirring. The resulting product was allowed to cool and then filtered with a 0.45 μm syringe filter for subsequent metal analysis with an inductively coupled plasma mass spectrometer (7500 cx ICP-MS, Agilent, Santa Clara, CA, USA).

Figure 2. The cylindrical steel reactor (Techinstro) internally coated with PTFE.

b. Low temperature metal extraction

The optimized conditions for hydrothermal leaching were used in the next experimental series. Keeping the HNO_3 concentration at 2 N and the L/S ratio at 1/10, the experiments were conducted at lower temperatures (25–45 °C), increasing the processing time (2–24 h), while flakes were used as the processing material. The effect of stirring was also tested in lower temperature experiments since stirring could not be performed with the hydrothermal reactors.

4. Results and Discussion

4.1. Composition of End-of-Life PV Panels

As seen in Table 2, the silicon content in the cells was 64.5–65.2% (*w*/*w*), while the silver content was 1.1–1.4% (*w*/*w*). Cell composition was in good agreement with the report by Theocharis et al. [20]. The aluminum content of the cells was about 5.5–7.2 times greater than the silver content. The silver content in the metallic ribbons was much higher, between 4.6% and 6.2% (*w*/*w*), which was attributed to the silver band attached to the PV ribbon for electrical conduction [34].

The mass composition (wt.%) of the panel components (excluding the mass of the backsheet, which was about 11% of the panel mass) is presented in Table 3, while the losses due to milling are calculated hereafter. Although the metal ribbons and cells accounted for 1–1.16% and 5.1–5.2% of the panel mass, respectively, the silver content of the metal ribbons was comparable to that of the cells due to the higher silver concentration.

The total mass loss due to milling was 8.19% (*w*/*w*). The milled sample (the mixture of cells and metal ribbons) was subjected to XRF analysis and the Ag mass loss in the sample was calculated to be 30%. In the powder sample, there were negligible mass losses for Si and Al, but there were significant losses for Cu, Sn and Pb. This could be attributed to the very fine particles lost in the dust [Cu (75%), Sn (66%), Pb (71%) and Ag (30%)]. Thus, mass loss due to milling was not proportional for all elements, and Ag loss was significant. This implies that leaching using panel flakes instead of powder may be preferable.

4.2. Hydrothermal Leaching of c-Si Panels

The hydrothermal leaching of Si panels revealed that the reaction time was the most important factor for Ag leaching, followed by HNO_3 concentration (within the range of the tested parameters). Pareto charts of significant factor terms and their interactions in response to leaching efficiency are shown in Figure 3. These charts show the absolute values of the standardized effects from largest to smallest. A reference line (dashed) is drawn to show which effects are statistically significant. The Pareto chart is used for decision-making as it shows the effects of independent variables on leaching efficiency. The basic principle of Pareto analysis is based on the 80/20 rule, meaning that 80% of the results come from 20% of the means or causes; thus, few factors (20%) are vital, and many factors (80%) are insignificant [35,36]. Significant terms are above the dashed red line, while non-significant terms are below the red line. The L/S ratio was the least important factor for both m-Si and p-Si panels. In addition, the temperature was not a statistically significant factor for either sample (m-Si and p-Si) and there were no significant interactions between the parameters. The analysis of variance of the model is presented in Table S1 (Supplementary Materials).

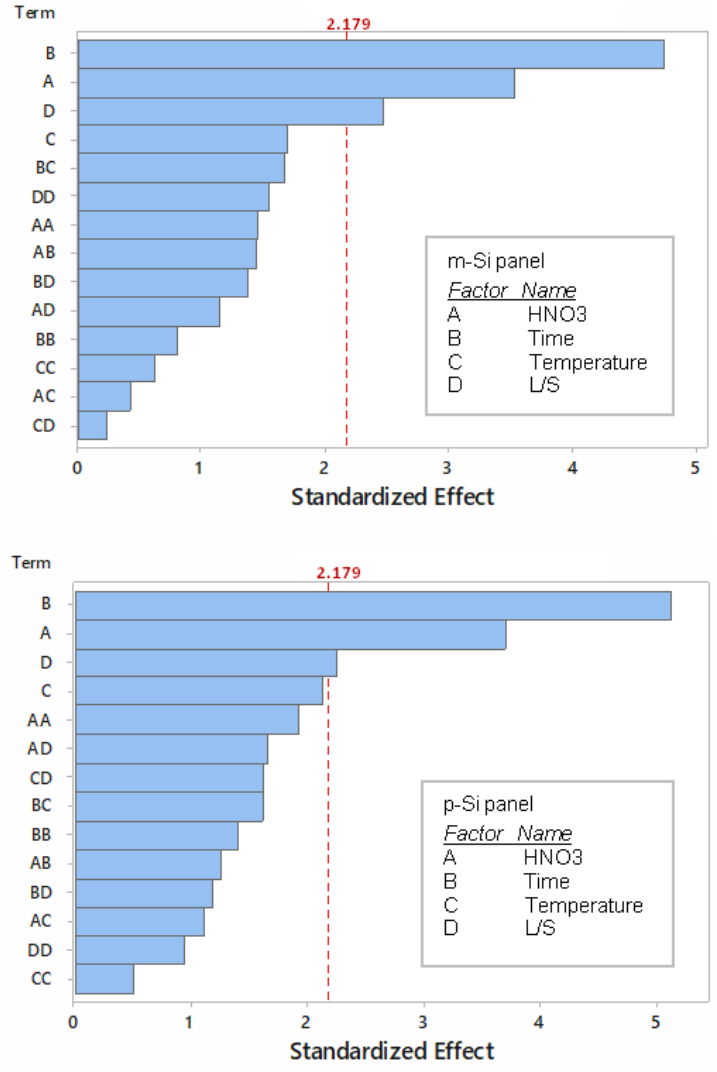

Figure 3. Pareto chart of standardized effects of the factors and interactions for Ag leaching from m-Si and p-Si panels.

Figure 4 presents the interaction between time and HNO_3 concentration regarding Ag leaching. Ag leaching efficiency increased significantly with increasing leaching time using 2 N HNO_3 for p-Si and m-Si. Figure 5 shows other factor interactions. Increasing the HNO_3 concentration and temperature also increased leaching efficiency; however, their effect was less significant than increasing the hydrothermal processing time. Reducing the L/S ratio increased the leaching yield, i.e., the concentration of Ag was higher. The main effects plots of temperature, time, L/S ratio and HNO_3 concentration on Ag leaching are depicted in Figure S1 (Supplementary Materials). The combination of temperatures, times, HNO_3 concentrations and L/S ratio in Ag leaching experiments resulted in leaching yields ranging from 0.12% to 74% for p-Si, while for m-Si, the efficiency of Ag leaching ranged between 5.7% and 66.2%. The highest Ag leaching yield was achieved at 2 N HNO_3, L/S = 10, 120 °C and 75 min. The lowest yield value was achieved at 1.5 N HNO_3, L/S = 15, 100 °C and 30 min. Based on the optimization obtained using mathematical equations defining the BBD/RSM, the optimized conditions to maximize Ag leaching (i.e., a 100% yield) through hydrothermal treatment are 2 N HNO_3, L/S = 10, 140 °C and 2 h leaching, which was experimentally validated.

Aluminum leaching was also investigated under the same conditions. The main effects plot for the parameters (HNO_3, time, temperature, and L/S ratio) revealed that Al leaching increased favorably with processing time and L/S ratio (Figure S2 Supplementary

Materials), while the other two factors were less significant. Efficient Al leaching was observed using 1 N HNO_3 under hydrothermal conditions. For m-Si and p-Si samples, the efficiency of Al leaching ranged from 23% to 88% and from 29% to 85%, respectively. The optimized conditions for maximum Al leaching were 2 N HNO_3, L/S = 10, 140 °C and 2 h leaching. In conclusion, Ag is the most valuable metal in PV panel waste; however, favorable Al leaching can be accomplished under the same conditions.

4.3. Conventional Leaching of Ag at Lower Temperatures

Since the elevated temperature of the hydrothermal process was not a statistically significant parameter for Ag leaching, further experiments were conducted at lower temperatures for comparison. In addition, as time was found to be an important factor, the effect of extending the leaching time was further investigated. The experiments were conducted at 25 °C and 45 °C, keeping the HNO_3 concentration at 2 N and the L/S at 10. The effect of stirring was further investigated.

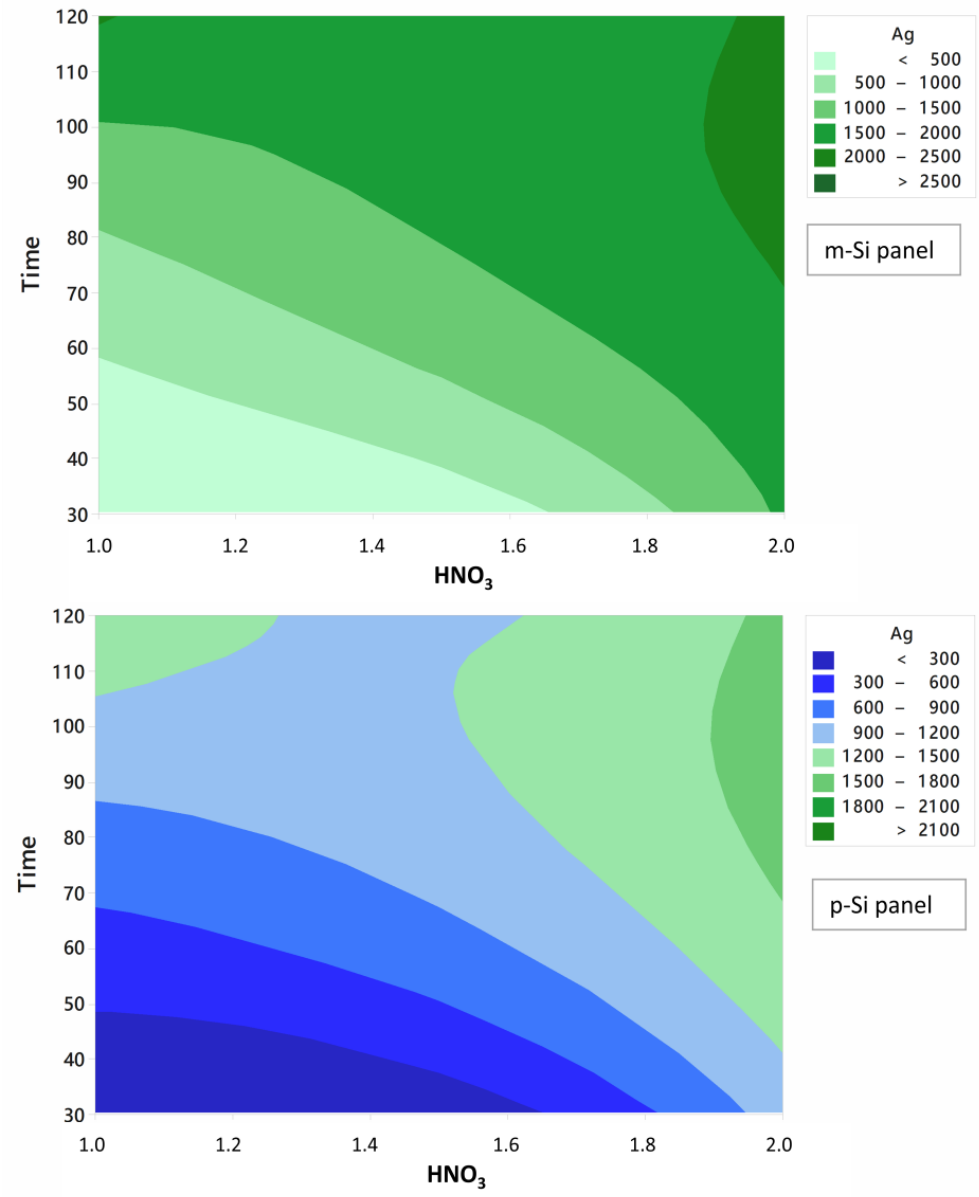

Figure 4. Fitted contour plots of Ag concentration vs. time and HNO_3 concentration for m-Si and p-Si panels.

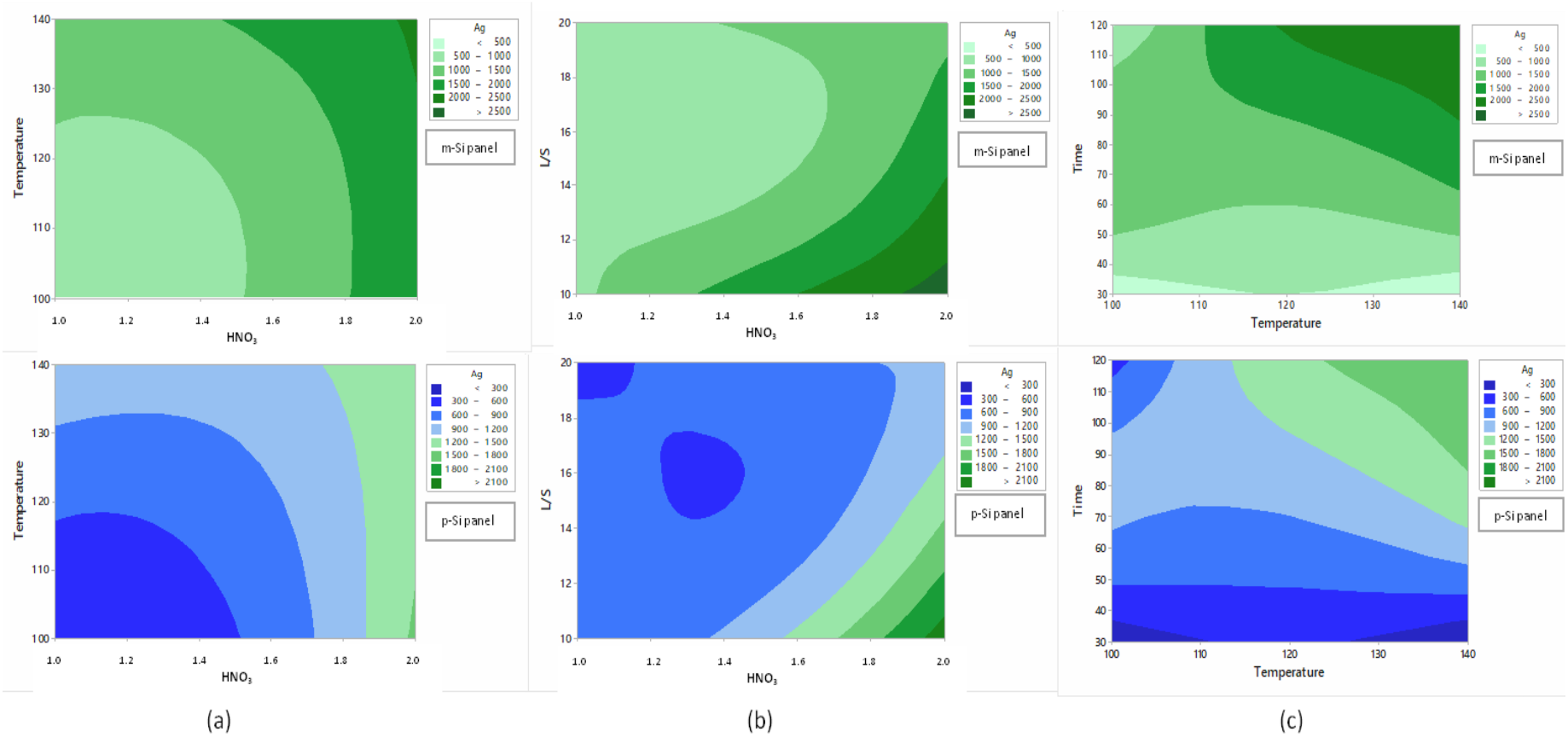

Figure 5. Fitted contour plots for m-Si and p-Si panels: (**a**) Ag concentration vs. temperature and HNO3; (**b**) Ag concentration vs. L/S and HNO_3; (**c**) Ag concentration vs. time and temperature.

The effect of stirring on Ag leaching was significant, with leaching efficiency increasing by 40% when stirring at 200 rpm (2 N HNO_3, L/S = 10, 45 °C, 2 h); thus, stirring was applied to all subsequent experiments at 25 °C and 45 °C (Figure S3 Supplementary Materials). The positive effect of stirring was ascribed to the access of metals to the leaching agent [33]. The effect of temperature is illustrated in Figure 6a for m-Si. It was observed that leaching with 2 N HNO_3 for 6 h at 45 °C had 80% efficiency, compared with 63.3% efficient at 25 °C; thus, the temperature of 45 °C was used in subsequent experiments. Next, leaching was performed at 45 °C for powder and flaked m-Si and p-Si panels. For m-Si panels, the maximum Ag leaching efficiency from flakes was 76.5% at 6 h; meanwhile, for p-Si panels, the leaching efficiency was 78% at 6 h (Figure 6b). Thus, the use of the powdered sample increased the leaching efficiency by 4.7–5.4%. Complete Ag leaching could not be achieved under low temperature conditions, even when the reaction time was increased to 24 h (2 N HNO_3, L/S = 10). For 24 h leaching, the Ag efficiency was 80.7% and 85.3% from m-Si and p-Si waste panels, respectively. However, Theocharis et al. [20] observed almost total leaching (100%) from PV flakes for 5 h leaching at 25 °C but with a 3 N HNO_3 concentration, while for PV powder, 100% leaching efficiency was achieved at 25 °C, 3 N HNO_3, for 2 h. Furthermore, Chen et al. [37] reported 99.4% Ag leaching efficiency at 80 °C with 5 N HNO_3 for 1 h.

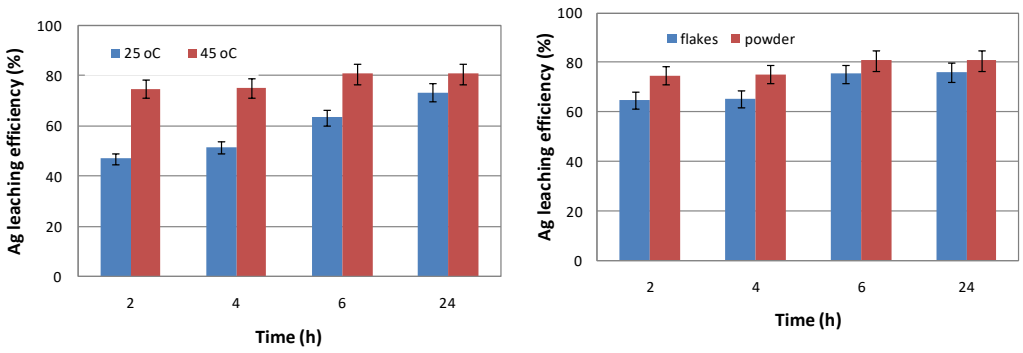

Figure 6. The effect of (**a**) temperature and (**b**) milling on Ag leaching (2 N HNO_3, L/S = 10, m-Si sample).

For Al, the leaching efficiency from the m-Si panel was 61.7% at 45 °C for 6 h (vs. 56.6% from p-Si panel) which compares to 44.7% efficiency in the m-Si panel at 25 °C for 6 h. However, for 24 h leaching, the efficiency was 61% at both 25 °C and 45 °C in the m-Si panel (Figure S4 Supplementary Materials). For the unpulverized sample, the m-Si panel leaching efficiency was 49% at 45 °C for 8 h (Figure S5 Supplementary Materials). Complete Al leaching was not achieved under low temperature conditions; however, it was favored under hydrothermal conditions. In the first case, the dissolution of Al may be partially inhibited by the formation of an aluminum oxide (Al_2O_3) layer on the surface and Al–Si compounds formed during acid treatment [38]. After acid leaching, Al can only be fully dissolved with NaOH [33]. Chen et al. [37] reported 76% Al leaching efficiency at 80 °C with 5 N HNO_3 for 1 h; however, Theocharis et al. [20] observed a 100% Al leaching yield after 2 h leaching at 25 °C with 3N HNO_3.

5. Conclusions

PV waste recycling is challenging due to the complexity of the PV structure and the tiny amounts of multiple elements that co-exist in its various components. In this study, hydrothermal leaching experiments were planned using response surface methodology with a Box–Behnken design. The Box–Behnken design effectively avoided the realization of the complete experimental design, which would otherwise make the process more demanding in terms of time and resources, yet without losing any information on the

effects of the parameters on the process. The hydrothermal leaching of Ag and Al was studied with the aim of developing an environmentally friendly process that could use weak acids, short leaching times and relatively low reaction temperatures. Before leaching, the fluoropolymer backsheet was manually removed and thermal degradation of the ethyl vinyl acetate (EVA) polymer was applied. The optimized hydrothermal process parameters were L/S = 10, 2 N HNO_3, 120 min and 140 °C. Under these parameters, Ag and Al were efficiently extracted. Since temperature was not a statistically significant parameter, further experiments were performed at lower temperatures to compare hydrothermal leaching to conventional low temperature processes. Under the low temperature leaching conditions, Ag could be leached using stirring and longer reaction times to generate a yield of 80.7–85%, while Al leaching was insufficient (at 56.6–61% efficiency) due to the formation of Al–Si compounds. Hydrothermal treatment favors the leaching of valuable metals; furthermore, it is more efficient and environmentally friendly than traditional leaching methods and may create financial benefits through the urban mining of PV waste.

Supplementary Materials: The following supporting information can be downloaded at: https://www.mdpi.com/article/10.3390/app13063602/s1. Table S1. Analysis of Variance of the model (Response surface methodology with a Box- Behnken design) for Ag leaching from (a) m-Si and (b) p-Si waste panel; Figure S1. The main effects plot for the parameters HNO_3, Time, Temperature and S/L ratio on Ag leaching from (a) m-Si and (b) p-Si waste panel; Figure S2. The main effects plot for the parameters HNO3, Time, Temperature and S/L ratio on Al leaching from m-Si waste panel; Figure S3. The effect of stirring on Ag leaching (p-Si panel, HNO_3 2N, S/L=1/10, 2 h, 45 °C); Figure S4. The effect of temperature on Al leaching (m-Si panel, HNO_3 2N, S/L=1/10); Figure S5. The effect of milling on Al leaching (m-S panel, HNO_3 2N, S/L=1/10, 45 °C).

Author Contributions: Conceptualization, E.K.; Methodology, A.G.; Validation, E.K., E.L. and G.K.; Investigation, E.K., E.L. and G.K.; Resources, E.K. and A.G.; Writing—original draft, E.K.; Writing—review & editing, E.K. and A.G.; Visualization, E.K.; Supervision, A.G. All authors have read and agreed to the published version of the manuscript.

Funding: This research received no external funding.

Institutional Review Board Statement: Not applicable.

Informed Consent Statement: Not applicable.

Conflicts of Interest: The authors declare no conflict of interest.

References

1. Weckend, S.; Wade, A.; Heath, G. *End-of-Life Management: Solar Photovoltaic Panels*; IRENA/IEA-PVPS: Abu Dhabi, United Arab Emirates, 2016; ISBN 978-92-95111-99-8. Available online: www.irena.org/publications/2016/Jun/End-of-life-management-Solar-Photovoltaic-Panels (accessed on 12 November 2022).
2. Farrell, C.C.; Osman, A.I.; Doherty, R.; Saad, M.; Zhang, X.; Murphy, A.; Harrison, J.; Vennard, A.S.M.; Kumaravel, V.; Al-Muhtaseb, H.; et al. Technical challenges and opportunities in realising a circular economy for waste photovoltaic modules. *Renew. Sustain. Energy Rev.* **2020**, *128*, 109911. [CrossRef]
3. Kastanaki, E.; Giannis, A. Energy decarbonisation in the European Union: Assessment of photovoltaic waste recycling potential. *Renew. Energy* **2022**, *192*, 1–13. [CrossRef]
4. Dias, P.; Javimczik, S.; Benevit, M.; Veit, H. Recycling WEEE: Polymer characterization and pyrolysis study for waste of crystalline silicon photovoltaic modules. *Waste Manag.* **2017**, *60*, 716–722. [CrossRef] [PubMed]
5. de Oliveira, L.S.S.; Lima, M.T.W.D.C.; Yamane, L.; Siman, R.R. Silver recovery from end-of-life photovoltaic panels. *Detritus* **2020**, *10*, 62–74. [CrossRef]
6. Hunt, A.J.; Matharu, A.S.; King, A.H.; Clark, J.H. The importance of elemental sustainability and critical element recovery. *Green Chem.* **2015**, *17*, 1949–1950. [CrossRef]
7. Tao, M.; Fthenakis, V.; Ebin, B.; Steenari, B.M.; Butler, E.; Sinha, P.; Corkish, R.; Wambach, K.; Simon, E.S. Major challenges and opportunities in silicon solar module recycling. *Prog. Photovolt. Res. Appl.* **2020**, *28*, 1077–1088. [CrossRef]
8. Huang, W.-H.; Shin, W.J.; Wang, L.; Tao, M. Recovery of valuable and toxic metals from crystalline-Si modules. In Proceedings of the IEEE 43rd Photovoltaic Specialists Conference (PVSC), Portland, OR, USA, 5–10 June 2016; pp. 3602–3605. [CrossRef]
9. Kuczyńska-Łażewskaa, A.; Klugmann-Radziemskaa, E.; Sobczakb, Z.; Klimczuk, T. Recovery of silver metallization from damaged silicon cells. *Sol. Energy Mater. Sol. Cells* **2018**, *176*, 190–195. [CrossRef]

10. Savvilotidou, V.; Gidarakos, E. Pre-concentration and recovery of silver and indium from crystalline silicon and copper indium selenide photovoltaic panels. *J. Clean. Prod.* **2020**, *250*, 119440. [CrossRef]
11. Klugmann-Radziemska, E.; Ostrowski, P. Chemical treatment of crystalline silicon solar cells as a method of recovering pure silicon from photovoltaic modules. Renew. *Energy* **2010**, *35*, 1751–1759. [CrossRef]
12. Shin, J.; Park, J.; Park, N. A method to recycle silicon wafer from end-of-life photovoltaic module and solar panels by using recycled silicon wafers. *Sol. Energy Mater. Sol. Cells* **2017**, *162*, 1–6. [CrossRef]
13. Dias, P.R.; Benevit, M.G.; Veit, H.M. Photovoltaic solar panels of crystalline silicon: Characterization and separation. *Waste Manag. Res.* **2016**, *34*, 235–245. [CrossRef]
14. Tanong, K.; Coudert, L.; Chartier, M.; Mercier, G.; Blais, J.F. Study of the factors influencing the metals solubilisation from a mixture of waste batteries by response surface methodology. *Environ. Technol.* **2017**, *38*, 3167–3179. [CrossRef]
15. Behera, S.K.; Meena, H.; Chakraborty, S.; Meikap, B.C. Application of response surface methodology (RSM) for optimization of leaching parameters for ash reduction from low-grade coal. *Int. J. Min. Sci. Technol.* **2018**, *28*, 621–629. [CrossRef]
16. Ferreira, S.L.C.; Bruns, R.E.; Ferreira, H.S.; Matos, G.D.; David, J.M.; Brandão, G.C.; da Silva, E.G.P.; Portugal, L.A.; dos Reis, P.S.; Souza, A.S.; et al. Box-Behnken design: An alternative for the optimization of analytical methods. *Anal. Chim. Acta* **2007**, *597*, 179–186. [CrossRef]
17. Zheng, X.; Zhu, Z.; Lin, X.; Zhang, Y.; He, Y.; Cao, H.; Sun, Z. A Mini-Review on Metal Recycling from Spent Lithium Ion Batteries. *Engineering* **2018**, *4*, 361–370. [CrossRef]
18. Xing, P.; Wang, C.; Wang, L.; Ma, B.; Chen, Y. Hydrometallurgical recovery of lead from spent lead-acid battery paste via leaching and electrowinning in chloride solution. *Hydrometallurgy* **2019**, *189*, 105134. [CrossRef]
19. Zhang, Z.; Liu, M.; Wang, L.; Chen, T.; Zhao, L.; Hu, Y.; Xu, C. Optimization of indium recovery from waste crystalline silicon heterojunction solar cells by acid leaching. *Sol. Energy Mater Sol. Cells* **2021**, *230*, 111218. [CrossRef]
20. Theocharis, M.; Pavlopoulos, C.; Kousi, P.; Hatzikioseyian, A.; Zarkadas, I.; Tsakiridis, P.E.; Remoundaki, E.; Zoumboulakis, L.; Lyberatos, G. An Integrated Thermal and Hydrometallurgical Process for the Recovery of Silicon and Silver from End-of-Life Crystalline Si Photovoltaic Panels. *Waste Biomass Valorization* **2022**, *13*, 4027–4041. [CrossRef]
21. Chen, W.-S.; Chen, Y.-J.; Lee, C.-H.; Cheng, Y.-J.; Chen, Y.-A.; Liu, F.-W.; Wang, Y.-C.; Chueh, Y.-L. Recovery of valuable materials from the waste crystalline-silicon photovoltaic cell and ribbon. *Processes* **2021**, *9*, 712. [CrossRef]
22. Yang, E.-H.; Lee, J.-K.; Lee, J.-S.; Ahn, Y.-S.; Kang, G.-H.; Cho, C.-H. Environmentally friendly recovery of Ag from end-of-life c-Si solar cell using organic acid and its electrochemical purification. *Hydrometallurgy* **2017**, *167*, 129–133. [CrossRef]
23. Lee, J.-K.; Lee, J.-S.; Ahn, Y.-S.; Kang, G.-H. Efficient Recovery of Silver from Crystalline Silicon Solar Cells by Controlling the Viscosity of Electrolyte Solvent in an Electrochemical Process. *Appl. Sci.* **2018**, *8*, 2131. [CrossRef]
24. Zheng, Q.; Shibazaki, K.; Ogawa, T.; Kishita, A.; Hiraga, Y.; Nakayasu, Y.; Watanabe, M. Continuous hydrothermal leaching of $LiCoO_2$ cathode materials by using citric acid. *React. Chem. Eng.* **2020**, *5*, 2148–2154. [CrossRef]
25. Zheng, Q.; Watanabe, M.; Iwatate, Y.; Azuma, D.; Shibazaki, K.; Hiraga, Y.; Kishita, A.; Nakayasu, Y. Hydrothermal leaching of ternary and binary lithium-ion battery cathode materials with citric acid and the kinetic study. *J. Supercrit. Fluids* **2020**, *165*, 104990. [CrossRef]
26. Yuxin, Z.; Ting, S.; Hongyu, C.; Ying, Z.; Zhi, G.; Suiyi, Z.; Xinfeng, X.; Hong, Z.; Yidi, G.; Yang, H. Stepwise recycling of Fe, Cu, Zn and Ni from real electroplating sludge via coupled acidic leaching and hydrothermal and extraction routes. *Environ. Res.* **2023**, *216*, 114462. [CrossRef]
27. Rao, S.; Wang, D.; Cao, H.; Zhu, W.; Duan, L.; Liu, Z. Hydrothermal oxidative leaching of Cu and Se from copper anode slime in a diluted H_2SO_4 solution. *Sep. Purif. Technol.* **2022**, *300*, 121696. [CrossRef]
28. Luo, M.; Liu, F.; Zhou, Z.; Jiang, L.; Jia, M.; Lai, Y.; Li, J.; Zhang, Z. A comprehensive hydrometallurgical recycling approach for the environmental impact mitigation of EoL solar cells. *J. Environ. Chem. Eng.* **2021**, *9*, 106830. [CrossRef]
29. Park, J.; Park, N. Wet etching processes for recycling crystalline silicon solar cells from end-of-life photovoltaic modules. *RSC Adv.* **2014**, *4*, 34823–34829. [CrossRef]
30. Fiandra, V.; Sannino, L.; Andreozzi, C.; Corcelli, F.; Graditi, G. Silicon photovoltaic modules at end-of-life: Removal of polymeric layers and separation of materials. *Waste Manag.* **2019**, *87*, 97–107. [CrossRef]
31. Badiee, A.; Ashcroft, I.A.; Wildman, R.D. The thermo-mechanical degradation of ethylene vinyl acetate used as solar panel adhesive and encapsulant. *Int. J. Adhes. Adhes.* **2016**, *68*, 212–218. [CrossRef]
32. Oliveira, M.C.C.; Diniz, A.S.A.C.; Viana, M.M.; Lins, V.F.C. The causes and effects of degradation of encapsulant ethylene vinyl acetate copolymer (EVA) in crystalline silicon photovoltaic modules: A review. *Renew Sustain. Energy Rev.* **2018**, *81*, 2299–2317. [CrossRef]
33. Kamberović, Ž.; Ranitović, M.; Korać, M.; Andjić, Z.; Gajić, N.; Djokić, J.; Jevtić, S. Hydrometallurgical Process for Selective Metals Recovery from Waste-Printed Circuit Boards. *Metals* **2018**, *8*, 441. [CrossRef]
34. Patcharawit, T.; Kansomket, C.; Wongnaree, N.; Kritsrikan, W.; Yingnakorn, T.; Khumkoa, S. Hybrid Recovery of Copper and Silver from PV Ribbon and Ag Finger of EOL Solar Panels. *Int. J. Power Energy Eng.* **2022**, *16*, 6. Available online: https://publications.waset.org/10012588/hybrid-recovery-of-copper-and-silver-from-pv-ribbon-and-ag-finger-of-eol-solar-panels (accessed on 12 November 2022).
35. Hu, X.-B.; Gu, S.-H.; Zhang, C.; Zhang, G.-P.; Zhang, M.-K.; Leeson, M.S. Finding all Pareto Optimal Paths by Simulating Ripple Relay Race in multi-objective networks. *Swarm Evol. Comput.* **2021**, *64*, 100908. [CrossRef]

36. Katsuaki, T. Pareto's 80/20 rule and the Gaussian distribution. *Phys. A Stat. Mech. Appl.* **2018**, *510*, 635–640.
37. Chen, W.-S.; Chen, Y.-J.; Yueh, K.-C.; Cheng, C.-P.; Chang, T.-C. Recovery of valuable metal from Photovoltaic solar cells through extraction. *IOP Conf. Ser. Mater. Sci. Eng.* **2020**, *720*, 012007. [CrossRef]
38. Šleiniūtė, A.; Urbelytė, L.; Denafas, J.; Kosheleva, A.; Denafas, G. Feasibilities for silicon recovery from solar cells waste by treatment with nitric acid. *Chemija* **2020**, *31*, 4287. [CrossRef]